The ADC for the VST Telescope: theory and preliminary test of the electromechanical system

Pietro Schipani, Jacopo Farinato, Carmelo Arcidiacono, Sergio D'Orsi, Luigi Ferragina, et al.

Pietro Schipani, Jacopo Farinato, Carmelo Arcidiacono, Sergio D'Orsi, Luigi Ferragina, Davide Fierro, Demetrio Magrin, Laurent Marty, Francesco Perrotta, Roberto Ragazzoni, Gabriele Umbriaco, "The ADC for the VST Telescope: theory and preliminary test of the electromechanical system," Proc. SPIE 7739, Modern Technologies in Space- and Ground-based Telescopes and Instrumentation, 773948 (20 July 2010); doi: 10.1117/12.856893

SPIE.

Event: SPIE Astronomical Telescopes + Instrumentation, 2010, San Diego, California, United States

The ADC for the VST telescope: theory and preliminary test of the electromechanical system

Pietro Schipani*[a], Jacopo Farinato[b], Carmelo Arcidiacono[c], Sergio D'Orsi[d], Luigi Ferragina[d], Davide Fierro[d], Demetrio Magrin[b], Laurent Marty[d], Francesco Perrotta[a], Roberto Ragazzoni[b], Gabriele Umbriaco[e]
[a]INAF – Osservatorio Astronomico di Capodimonte, Salita Moiariello 16, I-80131 Napoli, Italy
[b]INAF – Osservatorio Astronomico di Padova, Vicolo dell'Osservatorio 5, I-35122 Padova, Italy
[c]INAF – Osservatorio Astrofisico di Arcetri, Largo Enrico Fermi 5, I-50125 Firenze, Italy
[d]INAF – VSTCeN, Salita Moiariello 16, I-80131 Napoli, Italy
[e]INAF – Università degli Studi di Padova, Vicolo dell'Osservatorio 3, I-35122 Padova, Italy

ABSTRACT

The VST telescope is equipped with an Atmospheric Dispersion Corrector to counterbalance the spectral dispersion introduced by the atmosphere. The well known effect of atmospheric refraction is the bending of incoming light due to variable atmospheric density along the light path. This effect depends on the tangent of the zenith angle and also varies with altitude, humidity and wavelength. Since the magnitude of refraction depends on the wavelength, the resulting effect is not only a deviation of the light beam from its original direction but also a spectral dispersion of the beam. This effect can be corrected by introducing a dispersing element in the instrument. In the VST case the device that compensates for this effect is based on a set of four prisms in two cemented doublet pairs. The system provides an adjustable counter dispersion by counter-rotating the two pairs of prisms. The counter-rotating angle depends on the atmospheric dispersion, which is computed with an atmospheric model using both environmental data (temperature, pressure, humidity) and the telescope position. Two different approaches have been compared for the computations to cross-check the results. The electromechanical system has been assembled, tested and debugged prior to the shipping to Chile. This paper describes the atmospheric models used in the VST case and the most recent phases of work.

Keywords: Atmospheric Dispersion Compensation, Telescope, Prisms

1. INTRODUCTION

The atmospheric refraction is the bending of light due to the earth's atmosphere, making the source appear higher in the sky than it actually is (Fig. 1): it is a consequence of the wavelength-dependent index of refraction of the atmosphere. The light from celestial objects is continuously refracted on its way through the earth's atmosphere because it moves through a media with continuously varying refraction index (caused by the variations of pressure, temperature and water vapour concentration with height). As the refraction depends on the wavelength (blue light is refracted more than red light) the effect is a deviation of the light beam from its original direction, and also a spectral widening of the beam, with shorter wavelengths being more refracted than longer ones. The effect depends on the tangent of the zenith angle, being 0 at the zenith, and on altitude, humidity, and wavelength. At large zenith angles, the differential refraction between red and blue can be several arcsecs.

The device that compensates for this effect is called an Atmospheric Dispersion Corrector (ADC). The image of a star with a ground-based telescope without an ADC is a vertical spectrum, especially noticeable at large zenith angles. With an ideal ADC this same image shows no dispersion.

There are two basic requirements for an ADC:

- variable dispersion to compensate that of the atmosphere at a given zenith angle
- zero-deviation at some mean wavelength

*schipani@oacn.inaf.it

Modern Technologies in Space- and Ground-based Telescopes and Instrumentation, edited by Eli Atad-Ettedgui, Dietrich Lemke, Proc. of SPIE Vol. 7739, 773948 · © 2010 SPIE · CCC code: 0277-786X/10/$18 · doi: 10.1117/12.856893

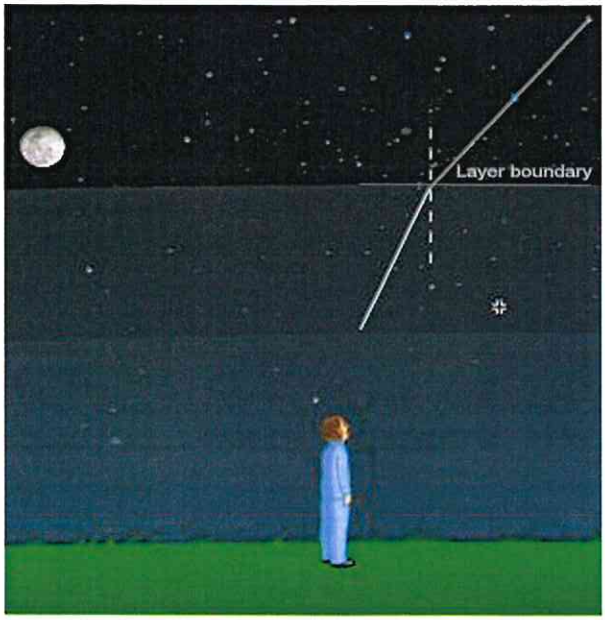

Fig. 1 – Refraction of air in the atmosphere

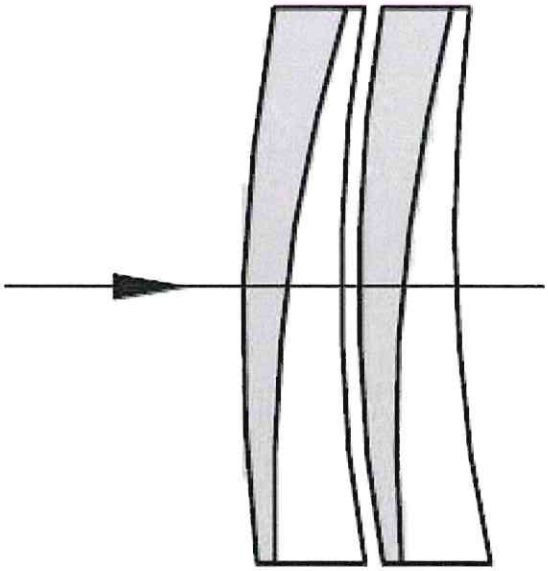

Fig. 2 – Conceptual scheme of VST ADC. Gray: Schott N-PSK3 glass; White: Schott LLF1 glass

Since this dispersion varies with the zenith angle, correction is usually implemented by installing two counter-rotating prisms to adjust the total refraction angle. Only two prisms cannot satisfy the zero-deviation condition. Thus, to satisfy the given requirements, an ADC is a set of four prisms in two cemented doublet pairs. If the two refracting prisms are made of two different glasses with the same refractivity at the central wavelength λo, the light passing through this pair of prisms at λo will have no deflection. In the VST case the two glasses for the prisms in each doublet are N-PSK3 and LLF1 arranged like in Fig. 2. The apex angles are in the same directions, corresponding to the maximum dispersion for this ADC arrangement. Further details on ADCs can be found in [1], [2], [3], [4], [5].

The dependence of the refractive indices of the two glasses on the wavelength is needed. The N-PSK3 glass refractive index is described by the Schott formula:

$$n^2_{glass1}(\lambda) = a_0 + a_1\lambda^2 + a_2\lambda^{-2} + a_3\lambda^{-4} + a_4\lambda^{-6} + a_5\lambda^{-8}$$

The LLF1 glass refractive index is described by the Herzberger formula:

$$n_{glass2}(\lambda) = A + BL(\lambda) + CL^2(\lambda) + D\lambda^2 + E\lambda^4 + F\lambda^6$$

where:

$$L(\lambda) = \frac{1}{(\lambda^2 - 0.028)}$$

Fig. 3 shows the dependence of refractive index on the wavelength for both glasses.

2. FILTER BANDWIDTHS

The atmospheric refraction depends on the wavelengths, that in VST are set by the filters of the OmegaCAM camera. As each filter has a different central wavelength and bandwidth, the atmospheric dispersion to be compensated depends on the filter. A set of possible OmegaCAM filters with their characteristics in terms of bandwidth and central wavelength is shown in Table 1.

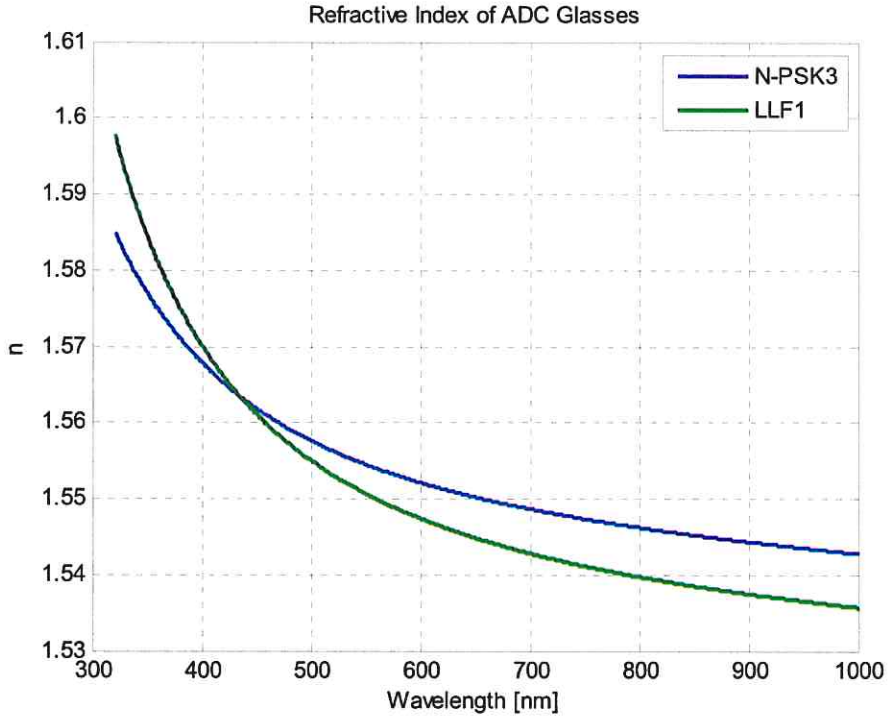

Fig. 3 – Refractive index of the two glasses

Filter Name	System	λ (nm)	Δλ (nm)
u'	SDSS	350	60
g'	SDSS	480	140
r'	SDSS	625	140
i'	SDSS	770	150
z'	SDSS	910	120
B	Johnson	440	100
B	Johnson	550	100
V	Strömgren	411	21

Table 1 - Filters

3. ATMOSPHERIC DISPERSION CALCULATION

The atmospheric dispersion is not measured; it is computed from an atmospheric model, using environmental data (temperature, pressure, humidity) and the telescope position. Different computational approaches are available in literature. Hereafter the atmospheric angular dispersion δ is computed by two atmospheric models, in order to cross-check the results.

3.1 First model

The model described in this section, derived from [6], is the baseline choice, and has been implemented in the VST Telescope Control Software. The refractive index of air n(λ, P, T) here depends on the wavelength λ, the barometric pressure P and the air temperature T. The refractive index of air at $P = 760$ mmHg and $T = 15$ °C is given by:

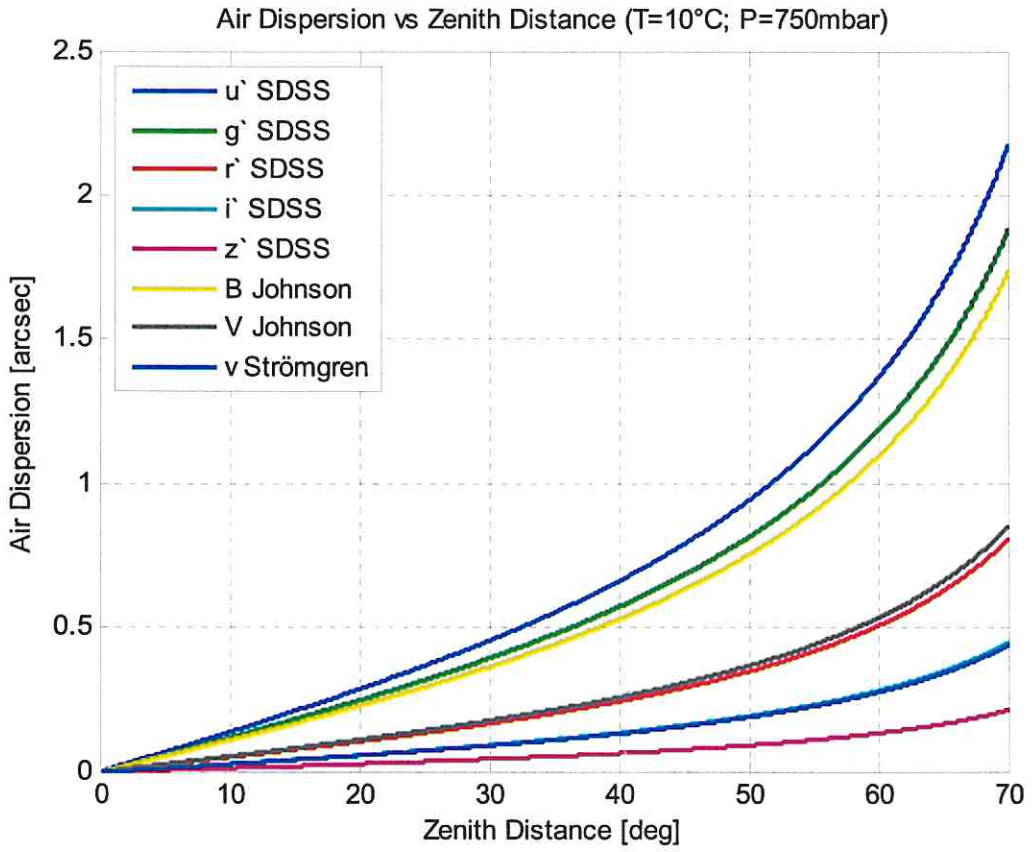

Fig. 4 – Atmospheric angular dispersion vs zenith angle

$$n(\lambda,760,15)-1=64.328+\frac{29498.1}{146-\left(\frac{1}{\lambda^2}\right)}+\frac{255.4}{41-\left(\frac{1}{\lambda^2}\right)}\cdot 10^{-6}$$

The refractive index, at generic pressure P and temperature T, is computed applying an appropriate scale factor:

$$n(\lambda,P,T)-1=\left(n(\lambda,760,15)-1\right)\frac{P\left[1+(1.049-0.0157T)P\times 10^{-6}\right]}{720.883(1+0.003661T)}$$

The refractive index difference in a given wavelength band $\left[\lambda_{\min},\lambda_{\max}\right]$ at pressure P=760mmHg and temperature T=0°C therefore is:

$$\Delta n=n\left(\lambda_{\min},760,0\right)-n\left(\lambda_{\max},760,0\right)$$

The atmospheric angular dispersion δ at pressure P=760mmHg and temperature T=0°C is proportional to the tangent of the zenith angle:

$$\delta\left(\lambda_{\min},\lambda_{\max},760,0,z\right)=\Delta n\tan(z)$$

The atmospheric angular dispersion in the bandwidth $\left[\lambda_{\min},\lambda_{\max}\right]$ for other P and T is computed applying a scale factor [7]:

$$\delta(\lambda_{\min},\lambda_{\max},P,T,z)=\frac{P}{760+2.9T}\Delta n\tan(z)$$

where the 2.9*T contribution makes an approximate allowance for the change of water-vapour content with temperature. This contribution compensates for the absence of an explicit dependence on the relative humidity in the formulas. Fig. 4 shows the atmospheric angular dispersion plotted against the zenith angle in the bandwidths defined by the filters.

3.2 Second model

The second model, implemented to cross-check the results, is described in [8]. This model is in agreement with the experimental data derived for EMMI instrument at La Silla ESO observatory [9]. Unlike in the previous model, here an explicit dependence on the relative humidity RH is introduced, i.e. the refractive index of air n(λ, P, T,RH) depends on the wavelength λ, the barometric pressure P, the air temperature T and the relative humidity RH. The saturation pressure of water P_S can be computed as:

$$P_S=-10474+116.43T-\text{-}0.43284\mathrm{T}^2+0.00053840\mathrm{T}^3$$

The partial pressure of water vapour P_w is computed by the relative humidity RH:

$$P_w=\frac{RH}{100}P_S$$

The partial pressure of waterfree dry air P_D is:

$$P_D=P-P_w$$

The contribution of the waterfree part of the air to the refraction of air is proportional to the density factor for dry air:

$$\mathrm{D_D}=\frac{\mathrm{P_D}}{\mathrm{T}}\left[1+\mathrm{P_D}\left(57.90\times10^{-8}\text{-}\frac{9.3250\times10^{-4}}{\mathrm{T}}+\frac{0.25844}{\mathrm{T}^2}\right)\right]$$

The contribution of the water vapour part to the refraction of air is proportional to the density factor for water vapour:

$$\mathrm{D_w}=\frac{\mathrm{P_w}}{\mathrm{T}}\left[1+\mathrm{P_w}\left(1+3.7\times10^{-4}\mathrm{P_w}\right)\left(-2.37321\times10^{-3}+\frac{2.23366}{T}-\frac{710.792}{T^2}+\frac{7.75141\times10^4}{T^3}\right)\right]$$

The simplified formula which finally results for the refractivity of moist air having partial pressures P_D and P_w of dry air containing 0.03%0 CO2, and of water vapour, respectively, is:

$$\mathrm{n}(\lambda,\mathrm{P,T,RH})\text{-}1=10^{-8}\left(2371.4+\frac{683939.7}{130-\sigma^2}+\frac{4547.3}{38.9-\sigma^2}\right)D_D$$

$$+\left(6487.31+58.058\sigma^2-0.7115\sigma^4+0.08851\sigma^6\right)D_w$$

where:

$$\sigma=\frac{1}{\lambda}$$

The refractive index difference in a wavelength band $[\lambda_{\min},\lambda_{\max}]$ at pressure P, temperature T and relative humidity RH therefore is:

$$\Delta n=n(\lambda_{\min},P,T,RH)-n(\lambda_{\max},P,T,RH)$$

The atmospheric angular dispersion in the bandwidth $[\lambda_{\min},\lambda_{\max}]$ is finally:

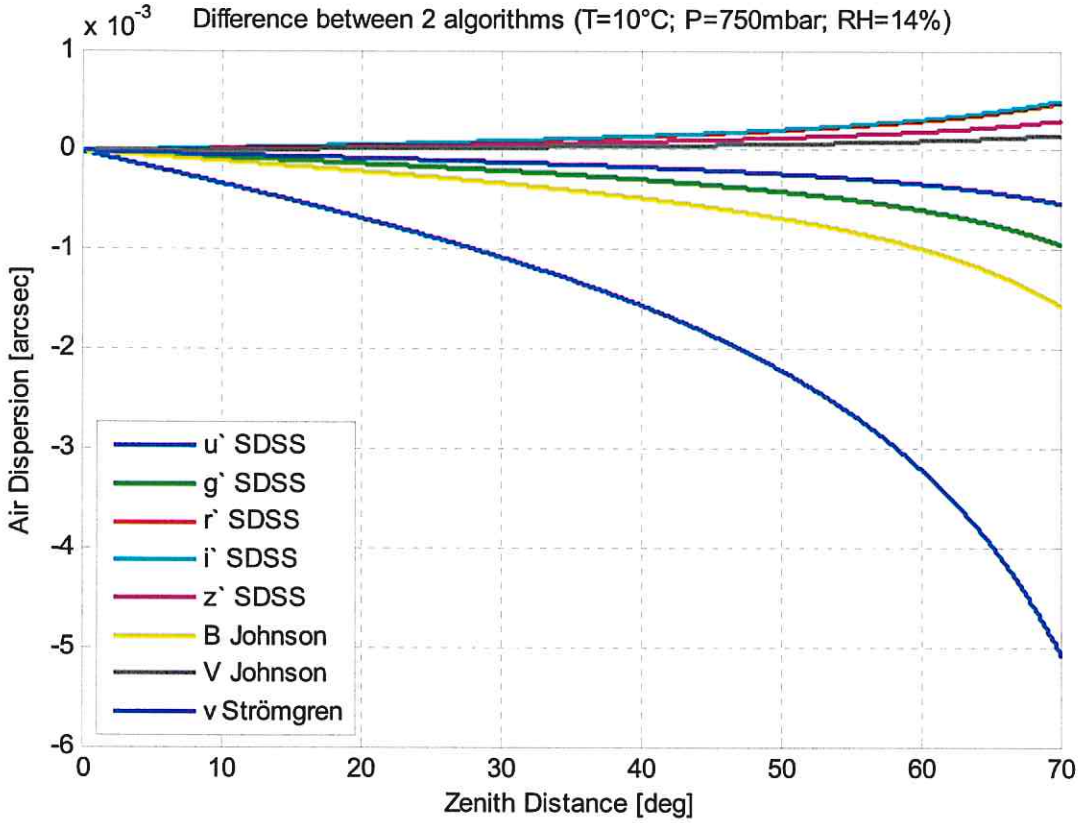

Fig. 5 – Difference between the two computation methods

$$\delta\left(\lambda_{\min},\lambda_{\max},P,T,z,RH\right)=\Delta n\tan(z)$$

Computing the atmospheric angular dispersion against the zenith angle in the bandwidths defined by the OmegaCam filters, the differences between the two methods are negligible, e.g. for most of the filters the difference is always less than 0.001 arcsec (Fig. 5). The first model (already used for VLT) has been taken in the final implementation.

4. CORRECTION USING THE ADC

Starting from the atmospheric dispersion formula, it is possible to compute the rotation of the prisms to counterbalance the effect of the atmosphere. The rotation angle for the ADC prisms comes from a straightforward computation based on geometric considerations. The adopted convention is that a null rotation corresponds to a null correction, and a 90° prisms doublet rotation corresponds to the maximum correction. Within this assumption, Fig. 6 represents the rotation ϕ of one prisms doublet against the zenith angle, computed for the filters in Table 1; the two doublets counter-rotate, hence the angular separation between them is 2ϕ. The maximum dispersion the system can physically achieve corresponds to a 90° prisms doublet rotation. For some filters (SDSS z', i', r') the atmospheric dispersion at very large zenith distances (greater than 60°) becomes higher than the maximum that can be corrected: in such rare cases the control system automatically applies the maximum possible dispersion, i.e. the prisms doublets are rotated to 90°.

5. CONTROL SYSTEM AND PRELIMINARY TESTS

The prisms motion control is based on stepper motors. Even though the stepper motor control system could work in open loop, providing the internal step counting as position feedback to the users, a closed position loop has been preferred and implemented, using Heidenhain encoders. The motion range is bounded by two hardware limit switches. During the initialization phase the absolute position is set finding the edge of a hardware switch, which can be the reference switch or one of the two hardware limits.

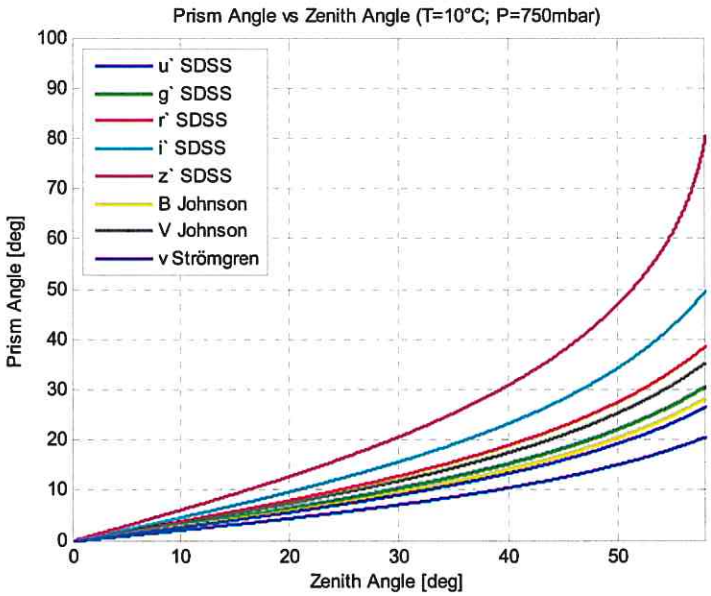

Fig. 6 – Prism rotation vs zenith angle

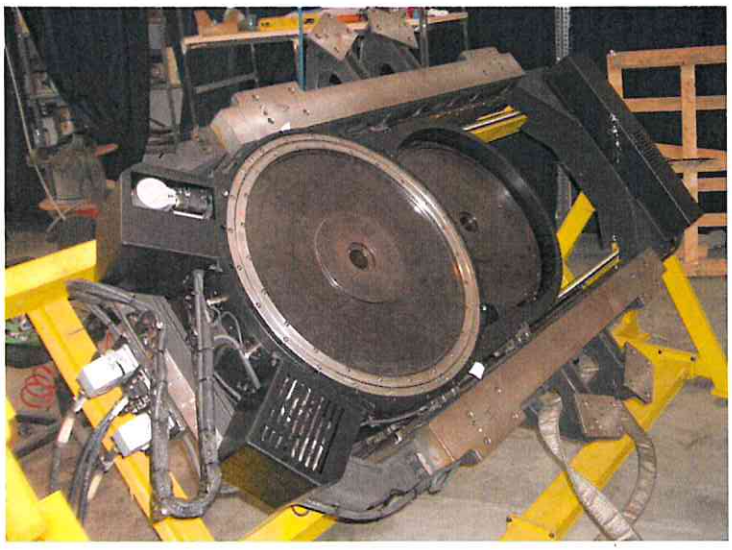

Fig. 7 – The ADC assembly installed on a tilting device to perform tests under realistic gravity conditions.

The motion control board is an ESO standard, the MAC4-STP VME bus motion control board from MACCON Gmbh, which can be operated with or without encoder. The VLT Common Software embeds the ESO's Motor Control Module, that supports the Maccon board and provides the engineering interfaces. The Maccon board continuously reprograms the number of steps to apply to the motor, in closed loop with the feedback coming from the encoder reading.

In the ESO standard configuration the Maccon MAC4-STP board is used in combination with an ESO custom amplifier board; the two boards are interconnected through their VME P2 connectors by an ESO custom backplane, and can serve up to 4 independent axes control. Nevertheless the ADC stepper motors work with 3A phase current, higher than the maximum current deliverable by the ESO amplifier board. Therefore the ESO amplifiers have been replaced with different drives, able to work at higher phase currents. A further advantage, with respect to the ESO amplifier board, was the availability off the shelf of stepper motor drive boards with a microstepping resolution configurable up to 1/128: this

allows to select a better resolution in motor positioning. Drive boards from LAM Technologies were selected; they did not fit in the ESO custom backplane, therefore a specific interface board was designed, that physically replaces the ESO amplifier in the Local Control Unit (LCU), and provides the communication between the ESO backplane and the LAM Technologies boards. With this solution, the standard ESO Maccon board and backplane have been saved, simplifying the maintenance of hardware and allowing to fully use the ESO's VLT Motor Control Module in the software.

Fig. 8 – The ADC assembly mounted on the backside of the primary mirror cell. Metallic dummies are installed in place of the prisms. The telescope is equipped with two sets of refracting elements which can be exchanged: the ADC (right side in the picture) and a field corrector (left).

With a few months of hard work in 2009, the ADC was completed and tested in the electromechanical parts by an INAF team, with the industrial support of Tomelleri srl.

The electromechanical part of the ADC system was tested under realistic gravity conditions, both on a tilting device (Fig. 7) and within the mirror cell (Fig. 8). Metallic dummies replaced the prisms during these tests. The positioning error of the prisms was measured; the system reliability was tested with repeated simulations of operating conditions. EMC tests were successfully performed on the control electronics cabinet. Further, the control software was tested and debugged up to the ADC handling in the telescope preset sequence.

6. CONCLUSIONS

The last phase of work in Italy has been described: the theory was assessed and cross-checked, the electromechanical system was improved and tested with dummies of the prisms, the control software was debugged and tested. This led to the shipment to Chile, where the integration of the telescope is ongoing. The installation of the glass prisms is forthcoming, as well as the tests on the sky.

REFERENCES

[1] Schroeder, D., Astronomical Optics 2nd Edition (Academic Press, 2000).
[2] Wilson, R., Reflecting Telescope Optics I (Springer, 2004).
[3] Bely, P. (ed.), The design and construction of large astronomical telescopes (Springer, 2003).
[4] Lemaitre, G. R., Astronomical optics and elasticity theory: active optics methods (Springer, 2009).
[5] Wynne, C.G., Worswick, S.P., "Atmospheric dispersion corrector at the Cassegrain focus", MNRAS 220, 657-670 (1986).
[6] Filippenko, A.V., "The importance of atmospheric differential refraction in spectrophotometry", PASP 94, 715-721 (1982).
[7] Allen, C.W., "Astrophysical Quantities", 3rd edition, Par. 55 "Athmospheric Refraction and Air Path" (1973).
[8] Owens, J.C., "Optical refractive index of air: dependence on pressure, temperature and composition", Appl.Opt. 6, 51-59 (1967).
[9] http://www.eso.org/gen-fac/pubs/astclim/lasilla/diffrefr.html